Journal of Colloid and Interface Science 210, 8–17 (1999)
Article ID jcis.1998.5776, available online at http://www.idealibrary.com on IDEAL®

Aggregation Behavior of Tyloxapol, a Nonionic Surfactant Oligomer, in Aqueous Solution

Oren Regev* and Raoul Zana†,[1]

*Department of Chemical Engineering, Ben-Gurion University, 84105 Beersheva, Israel; and †Institut C. Sadron (CNRS), 6 rue Boussingault, 67000 Strasbourg, France

Received March 26, 1998; accepted July 29, 1998

The aggregation behavior of Tyloxapol, a nonionic surfactant oligomer with a repeating unit close to Triton X-100 (TX100), and a maximum degree of polymerization of about 7, has been investigated in aqueous solution by means of fluorescence probing, time-resolved fluorescence quenching (TRFQ) and transmission electron microscopy at cryogenic temperature (cryo-TEM). The plot of the pyrene fluorescence intensity ratio I_1/I_3 against the Tyloxapol concentration shows no clear evidence of a critical micelle concentration contrary to TX100. Nevertheless, the fitting of these data, assuming a partition of pyrene between Tyloxapol aggregates and water, yields cmc values in the micromolar range, i.e., about a hundred times lower than for the "monomer" TX100. The values of I_1/I_3 at high surfactant concentrations indicate that Tyloxapol micelles provide pyrene a less polar environment than TX100 micelles. The use of the viscosity-sensitive probe 1,3-dipyrenylpropane indicates that the microviscosity of Tyloxapol micelles is quite high, three to four times larger than that for TX100 micelles, and decreases rapidly with increasing temperature. Also the microviscosities of both TX100 and Tyloxapol micelles are larger than those for the micelles of the nonionic ethoxylated surfactant $C_{12}E_9$. The aggregation numbers of Tyloxapol and of TX100 micelles measured using TRFQ increase with temperature, with the Tyloxapol micelles being smaller than the TX100 micelles. Cryo-TEM shows that the Tyloxapol micelles remain spheroidal up to a concentration of about 10 wt%. At 15 wt%, some regions of ordered elongated micelles are also observed which may be the precursors of the hexagonal phase known to occur at about 35 wt%.

Key Words: nonionic surfactant oligomer; Triton X-100; Tyloxapol; aggregation in aqueous solution; cmc; micelle shape; micelle microviscosity.

INTRODUCTION

In recent years a new class of surfactants which can be broadly referred to as surfactant oligomers has attracted increasing interest (1–5). Surfactant oligomers are made up of two or more amphiphilic moieties connected at the level of, or very close to, the head groups by a spacer group. The surfactant dimers, also referred to as gemini surfactants (2), have been the most investigated. The interest in surfactant dimers and oligomers is due to the fact that they are characterized by much lower critical micelle concentration (cmc) values and much stronger surface tension lowering action than the corresponding conventional (monomeric) surfactants (1–5). These two properties determine most uses of surfactants in formulations. Surfactant trimers and tetramers are characterized by even lower cmc values than surfactant dimers (6–8). The work on surfactant dimers and oligomers has been recently reviewed (3–5). Thus far, the reported studies have essentially concerned cationic and anionic surfactant dimers. There has been no report on the properties of nonionic surfactant oligomers, probably because of difficulties in their synthesis. However, a nonionic surfactant oligomer, referred to as Tyloxapol, has been synthesized and described (9, 10) and can be obtained from chemical manufacturers. Tyloxapol is very close to being an oligomer of the much investigated Triton X-100 (TX100; see chemical structures in Scheme 1). The micelle formation by Tyloxapol and the phase diagrams of Tyloxapol/water and Tyloxapol/TX100/water mixtures have been investigated (11–13). In view of our current interest in surfactant oligomers and the availability of Tyloxapol we decided to investigate its aggregation behavior in aqueous solution and to compare it to that of its monomer, TX100. For this purpose we made use of fluorescence probing using the probes pyrene (cmc, micelle polarity) and 1,3-dipyrenylpropane (micelle microviscosity) (14–16). We also used time-resolved fluorescence quenching (micelle aggregation numbers) (17–20) and transmission electron microscopy at cryogenic temperature (direct imaging of the aggregates in the surfactant solutions) (21). The results reveal important differences between the properties of the micelles of Tyloxapol and TX100 and also between their aggregation behaviors.

EXPERIMENTAL

Materials

The sample of TX100 (Aldrich Chemicals, Europe) was used as received. A sample of Tyloxapol (Sigma) was extensively dialyzed against water using dialysis bags with a cutoff of about 1500 Da and the surfactant was recovered by extensive vacuum rotatory evaporation first under 15 mm mercury

[1] To whom correspondence should be addressed.

0021-9797/99 $30.00

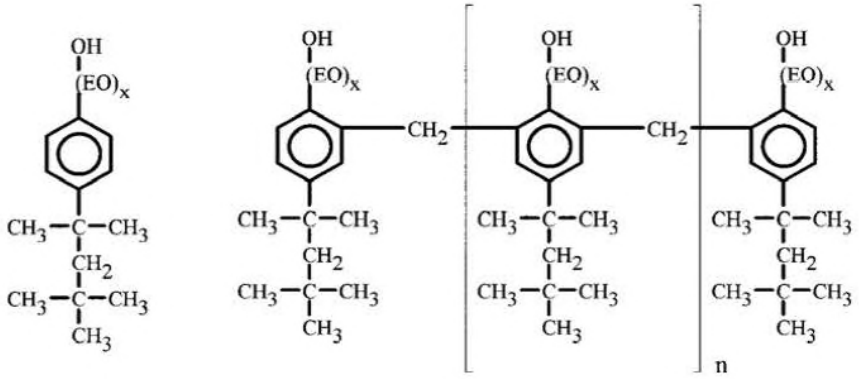

Triton X-100 Tyloxapol

x = 9-10 x = 8-10 n < 6

SCHEME 1. Chemical structures of Triton X-100 and of Tyloxapol (EO= $-CH_2CH_2O-$).

then under 1 mm mercury, at 40°C. The water content of the samples of raw and dialyzed Tyloxapol and of TX100 were measured using Karl–Fisher titration and found to be below 1 wt%. The concentrations given below have been corrected for that water content. The raw Tyloxapol was examined by size exclusion chromatography (solvent: tetrahydrofuran; four columns filled with beads of polystyrene cross-linked by divinylbenzene, of diameter 10 μm and of pore sizes 5, 10, 50, and 100 nm; detection: UV absorption or index of refraction). The chromatogram is shown in Fig. 1. Using the method reported in (22), this chromatogram was decomposed in a sum of four components corresponding to the monomer, dimer, trimer, and higher oligomers with percentages in weight of about 4.4, 10, 16.9, and 68.7, respectively (Fig. 1). The nonionic surfactant nonaethyleneglycol monododecyl ether ($C_{12}E_9$) was purchased from Fluka and used as received. The clouding temperatures of aqueous solutions of $C_{12}E_9$, TX100, and Tyloxapol at a concentration of 3 wt% were found to be 83 ± 0.5, 65.9 ± 0.2, and 90 ± 1°C, respectively.

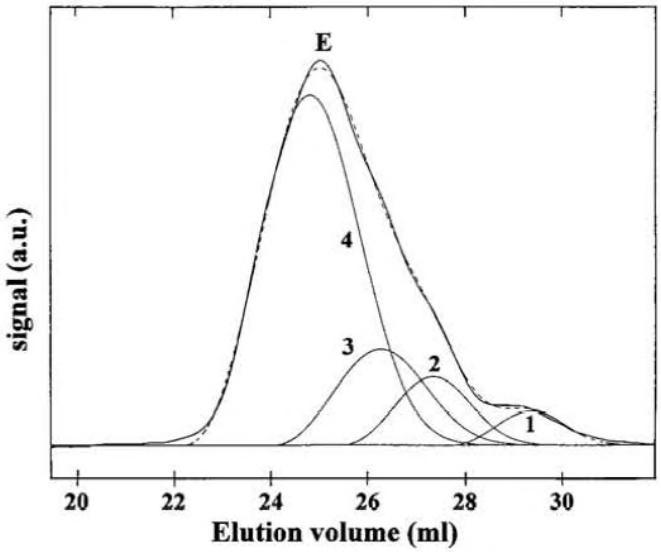

FIG. 1. Chromatogram of a 3 wt% solution of raw Tyloxapol in tetrahydrofuran. The signal (ordinate scale) is proportional to the refractive index of the eluted solution. The chromatogram has been analyzed according to the method in Ref. (22). Curve E is the experimental chromatogram. Curves 1, 2, 3, and 4 correspond to the monomer, dimer, trimer, and higher oligomer, respectively. The broken line curve is the sum of curves 1 to 4.

The fluorescence probes pyrene (purified by zone melting) and 1,3-dipyrenylpropane (DPP, from Molecular Probes, used without further purification) were the same as in previous studies (7). The quenchers of the pyrene fluorescence used for aggregation number determinations were dimethylbenzophenone (DMBP) (23) and tetradecylcyanopyridinium chloride (TCNPC) (24).

Water purifed using a Millipore Milli-RO 3Plus (resistance >18 mΩ) was used for the preparation of all solutions. The surfactant concentrations are expressed in wt% or in mol/L on the basis of molecular weights of 624 g/mol for TX100 and 636 g/mol for the repeating unit of Tyloxapol. These values assume an average of 9.5 ethoxy units per molecule or repeating unit (11–13).

Methods

Spectrofluorometry. The pyrene emission spectra were recorded using a Hitachi F4010 spectrofluorometer and used to obtain the ratio I_1/I_3 of the intensities of the first and third vibronic peaks in the emission spectra of pyrene solubilized in the micellar solutions. The excitation wavelength was set at 335 nm. For conventional surfactants the variation of I_1/I_3 with the surfactant concentration C permits one to obtain the cmc. In addition, the value of I_1/I_3 at $C \gg$ cmc gives a measure of the polarity sensed by pyrene at its micelle solubilization site (14, 15).

The emission spectra of DPP were recorded using the same spectrofluorometer in the range from 350 and 550 nm, using an excitation wavelength of 346 nm. These spectra showed an

emission due to the monomeric form of DPP in the range 360–400 nm with four vibronic peaks (I_M, intensity of the first peak located near 378 nm) and a broad emission maximum arising from the excimer form of DPP, centered at 485–490 nm (intensity I_E). The product of the intensity ratio I_M/I_E by fluorescence lifetime τ_E of the DPP excimer is proportional to the microviscosity of the surrounding medium (25, 26). The intensities I_M and I_E were measured using air-saturated solutions. The lifetimes in the same solutions were measured using a single photon counting apparatus (23, 24) at an excitation wavelength of 335 nm and monitoring the emission using a high-pass Kodak gelatin filter 4 ($\lambda > 460$ nm).

Time-resolved fluorescence quenching. We attempted to measure the aggregation numbers of Tyloxapol and TX100 micelles in aqueous solution using the time-resolved fluorescence quenching method (TRFQ) (15, 17–20) with pyrene as the fluorescent probe and DMBP or TCNPC as quenchers. The fluorescence decay curves were recorded using the same single photon counting apparatus which included a Type 7450 EGG-Ortec multichannel analyzer with a time base of 1024 channels (23, 24). As usual, the pyrene concentration was adjusted to be of about 1 to 2% of the micelle molar concentration, $[M]$, whereas the quencher molar concentration, $[Q]$, was adjusted to be close to $[M]$ (i.e., an average of one quencher per micelle). Prior to each experiment, the solutions investigated were deaerated by three successive freeze–pump–thaw cycles. The following fluorescence decay equations (17–20) were fitted to the experimental fluorescence decay curves of pyrene in the absence and in the presence of the quencher, respectively, using a weighted least-squares procedure (23, 24):

$$I(t) = I(0)\exp(-t/\tau) \quad [1]$$

$$I(t) = I(0)\exp\{-A_2t - A_3[1 - \exp(1 - A_4t)]\}. \quad [2]$$

In these equations $I(0)$ and $I(t)$ are the fluorescence intensities at time 0 and t, τ is the pyrene excited state lifetime in the absence of the quencher, and A_2, A_3, and A_4 are three fitting parameters. The micelle aggregation number, N, the rate constant for intramicellar quenching, k_Q, and the rate constant for probe and/or quencher exchange between micelles, k_e, may then be determined from

$$N = A_3\{(C - \text{cmc})/[Q]\}[1 + \epsilon]^2 \quad [3]$$

$$k_Q = A_4/[1 + \epsilon] \quad [4]$$

$$k_e = A_4 - k_Q = A_4\epsilon/(1 + \epsilon), \quad [5]$$

where C is the surfactant concentration in mole per dm^3 (15, 17–20), with

$$\epsilon = (A_2 - \tau^{-1})/A_3A_4. \quad [6]$$

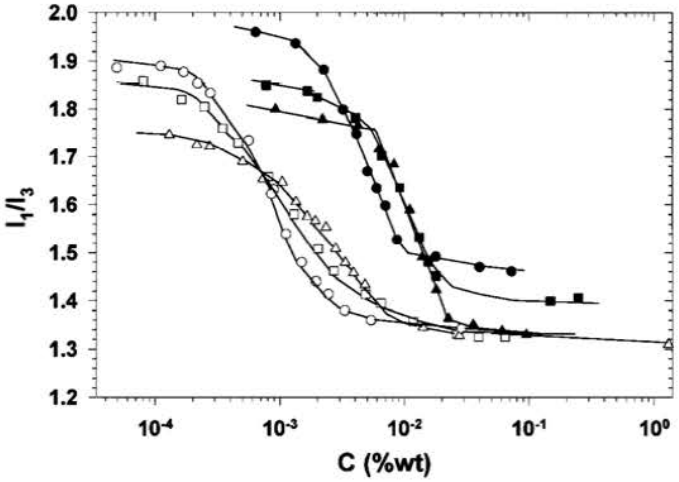

FIG. 2. Variations of I_1/I_3 with the surfactant concentration at 10°C (○, ●), 25°C (□, ■), and 40°C (△, ▲) for Tyloxapol (○, △, □) and TX100 (●, ▲, ■). The solid lines going through the data points are only guides to the eye.

The overall error on the aggregation number is estimated to be of ±10%.

Cryo-transmission electron microscopy (cryo-TEM). The specimens are prepared by blotting a 5-μl drop of the sample on a lacey carbon substrate (300 mesh, Ted Pella Inc.) in a controlled environment vitrification system (CEVS) (27), where temperature is controlled by a bulb and relative humidity is kept above 95% by a wet sponge to prevent sample evaporation. The specimen is blotted by a filter paper, resulting in the formation of a very thin sample film suspended over the grid, which is then vitrified very quickly in liquid ethane maintained at the liquid nitrogen temperature, 83 K (−190.15°C). The CEVS operation retains the original composition of the sample so that the original microstructures remain unaltered in the vitrified specimen. The vitrified specimen is then transferred by means of a Gatan cryoholder into a JEOL 1200EXII electron microscope operating at 100 kV in the conventional TEM mode with nominal underfocus of about 4 μm. The images are recorded at 83 K on SO-163 film. The low-dose mode of the electron beam is used to reduce radiation damage by the electron beam.

RESULTS AND DISCUSSION

The cmc and Micelle Micropolarity

Figure 2 shows the variations of the I_1/I_3 ratio with the surfactant concentration, C, for Tyloxapol and TX100 at 10, 25, and 40°C. The I_1/I_3 vs C plots for the raw and dialyzed samples of Tyloxapol were determined at 25°C and found to be coincident. This is not surprising in view of the very low fraction of monomer (4%) contained in the raw sample and which may be eliminated by dialysis. All of the measurements below refer to the raw sample. In all instances the intensity ratio shows a sigmoidal

decrease upon increasing C, revealing that pyrene goes from a hydrophilic to a hydrophobic environment. The latter is provided by surfactant aggregates when present in the solution with a sufficient volume fraction to solubilize pyrene. The two sets of results show important differences.

First, for Tyloxapol, the concentration range where most of the decrease of I_1/I_3 occurs is about 10-fold lower than that for TX100, showing that this surfactant oligomer provides pyrene with hydrophobic microdomains at a much lower concentration than its monomer. The cmc range of TX100 is seen to be around 0.01 wt%, i.e., 0.15 mM. The cmc of TX100 can be obtained using two approaches.

1. It is taken as the concentration corresponding to the intercept of the extrapolations of the high concentration part and of the rapidly varying part of the I_1/I_3 vs C plot (28). The cmc values are then found to be 0.012, 0.024, and 0.024 wt% which is about 0.19, 0.38, and 0.38 mM at 10, 25, and 40°C, respectively.

2. For several ionic and nonionic surfactants with the cmc in the 0.1 mM range the comparison of the electrical conductance or surface tension vs C plots and of the I_1/I_3 ratio vs C plots showed that the cmc, obtained for the conductance or surface tension plots (true cmc), closely corresponds to the concentration at the inflection point of the I_1/I_3 ratio vs C plot (29–31). This concentration is also very close to that at mid-decrease of the I_1/I_3 ratio. Using this procedure, the TX100 cmc values were found to be 0.05, 0.10, and 0.12 wt% (that is, 0.08, 0.16, and 0.19 mM) at 10, 25, and 40°C, respectively.

The cmc of TX100 has been reported to be between 0.25 and 0.27 mM at 25°C (32–34), a value between the ones given above at this temperature.

The second difference between Tyloxapol and TX100 is that the decrease of I_1/I_3 is much less steep for the former, stretching over nearly two decades of concentration for Tyloxapol against about one decade for TX100. In addition, there is no really sharp change at the end of the decrease for Tyloxapol, contrary to TX100. This complicates the determination of the "cmc" for Tyloxapol. Indeed, pyrene reports a partly hydrophobic environment already at a concentration of, say, 3×10^{-4} wt% (i.e., 5×10^{-6} M). However, the cmc, if it exists, may be located at an even lower concentration. Indeed at such a low amphiphile concentration the volume of the hydrophobic pseudo-phase is very small and a significant fraction of pyrene remains in the water, thereby reporting a partly aqueous environment even at concentrations above the cmc. The I_1/I_3 plots for Tyloxapol look very much like those characterizing systems with very low or zero cmc, where pyrene is progressively partitioned into hydrophobic aggregates, as the concentration of the amphiphile is increased (35). In such systems, the experimental fluorescence intensity ratio can be written in the form (35)

$$I_1/I_3 = (I_1/I_3)_{Ag} + [(I_1/I_3)_W - (I_1/I_3)_{Ag}]/[1 + K(C - \text{cmc})], \quad [7]$$

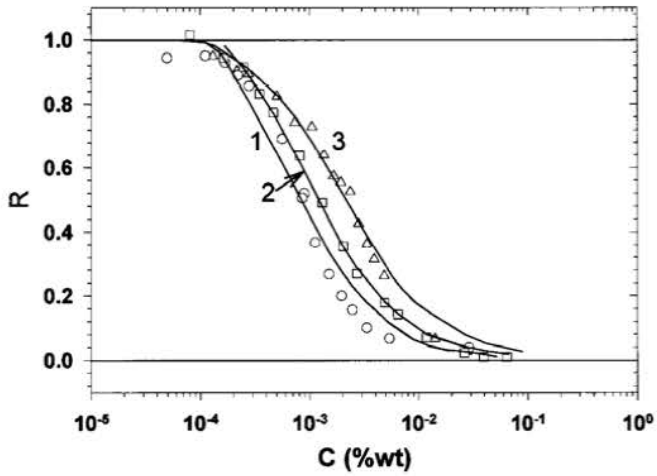

FIG. 3. Variations of the normalized fluorescence intensity ratio R with the surfactant concentration for Tyloxapol at 10°C (○), 25°C (□), and 40°C (△). The curves in solid lines 1, 2, and 3 have been calculated using Eq. [8] with the values K = 1434, 934, and 480 (wt%)$^{-1}$, and cmc = 1.1×10^{-4}, 1.4×10^{-4}, and 0.7×10^{-4} wt%, at 10, 25 and 40°C, respectively.

where $(I_1/I_3)_W$ and $(I_1/I_3)_{Ag}$ are the values of the intensity ratio in water and in the aggregate (that is, at $C \gg$ cmc), and K is an apparent binding constant of pyrene to the aggregates (K/55.5 is in fact the partition coefficient of pyrene between the hydrophobic domains considered as a pseudo-phase and water). The data in Fig. 2 have been normalized and replotted in Fig. 3 as R against C using a semi-logarithmic scale for the concentration, with R given by

$$R = [I_1/I_3 - (I_1/I_3)_{Ag}]/[(I_1/I_3)_W - (I_1/I_3)_{Ag}] = 1/[1 + K(C - \text{cmc})]. \quad [8]$$

The quantity R varies between 1 and 0 upon increasing C. It represents the fraction of pyrene solubilized in the aggregates. Its variation with log C is an S-shaped curve and $R = 0.5$ for $C - \text{cmc} = 1/K$. The R vs log C plots permit an easier comparison between surfactants of differing $(I_1/I_3)_{Ag}$ and also an easy visualization of the quality of the fit of Eq. [8] to the data. The plots 1–3 have been calculated using Eq. [8] with appropriate values of the binding constant and of the cmc given in the legend to Fig. 3. These plots are seen to provide a good fit for the Tyloxapol results at 25 and 40°C. The fit is somewhat less satisfactory at 10°C. The differences which may exist between the calculated curves and the data have been discussed and attributed to the large change of pyrene concentration in the aggregates at concentrations close to the cmc (35). The cmc values thus obtained are very inaccurate, around 10^{-4} wt%, which is 1.6 μM, at the three temperatures investigated. This value is very low, much lower than that for TX100. However, our results do not permit one to conclude whether the aggregates capable of binding pyrene in Tyloxapol solutions result from an aggregation of Tyloxapol around the pyrene mole-

cules, or reflect the solubilization or binding of pyrene to single Tyloxapol molecules which would be able to form intramolecular micelles, or arise from a true intermolecular association of Tyloxapol molecules as for normal amphiphiles at above the cmc. In the latter case our cmc value would be much smaller than that advanced by Westesen and Koch (12). Note that ionic surfactant oligomers have consistently been found to have much lower cmc values than the corresponding monomers. A similar behavior is expected for Tyloxapol with respect to TX100.

The third difference between TX100 and Tyloxapol is that at $C \gg$ cmc, as the temperature is decreased from 40 to 10°C, the value of I_1/I_3 increases from about 1.32 to 1.44 for TX100, but remains nearly constant at about 1.32 for Tyloxapol. At 25°C the values of I_1/I_3 are 1.32 and 1.4 for Tyloxapol and TX100, respectively, indicating that the micelles of Tyloxapol provide pyrene with an environment of lower polarity than TX100 micelles (14, 15). However, at 40°C, Tyloxapol and TX100 micelles are characterized by about the same value of I_1/I_3.

Microviscosity

The values of the DPP excimer lifetime and of the ratio I_M/I_E were determined for Tyloxapol and TX100 solutions at different concentrations and temperatures. We did not attempt to calculate absolute microviscosities from the results. Indeed this involves the use of a calibration plot (plot of $\tau_E I_M/I_E$ vs viscosity for a series of liquids of known viscosity) and the microviscosities thus obtained depend on the calibration curve used (36). Since we were essentially interested in comparing the micellar microviscosities of Tyloxapol and of its monomer TX100, all the results below concern the values of the product $\tau_E I_M/I_E$ which is referred to as microviscosity even though it is realized that it is only proportional to the microviscosity. At the outset it should be stated that the measurements of I_M/I_E for Tyloxapol solutions at temperatures below 40°C were difficult

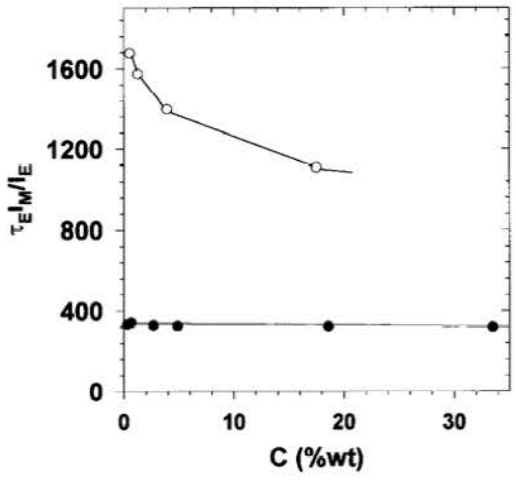

FIG. 4. Variations of the micelle microviscosity with the surfactant concentration for Tyloxapol (○) and TX100 (●) at 45°C.

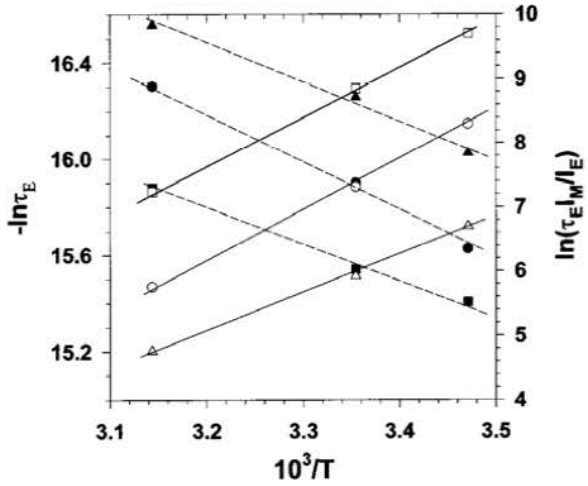

FIG. 5. Variations of the micelle microviscosity (solid lines) for Tyloxapol (□), TX100 (○), and $C_{12}E_9$ (△), and corresponding variations of the lifetime of the DPP excimer (broken lines) for Tyloxapol (■), TX100 (●), and $C_{12}E_9$ (▲), with temperature.

because of the extremely low values of the excimer intensity which reflect extremely large values of the microviscosity. The $\tau_E I_M/I_E$ values for Tyloxapol solutions below 40°C must be considered lower bound values.

Figures 4 and 5 show the variations of $\tau_E I_M/I_E$ with concentration and temperature (T), respectively, for Tyloxapol and TX100. In all instances the microviscosity of Tyloxapol aggregates is larger than that of TX100. A similar difference has been found between the microviscosity values of ionic surfactant oligomers and their corresponding monomers (7). Figure 4 shows that the microviscosity is nearly independent of the TX100 concentration but decreases somewhat as the Tyloxapol concentration is increased. Figure 5 shows that the microviscosity of both Tyloxapol and TX100 aggregates decreases steeply as the temperature increases. In the semi-logarithmic representation adopted in Fig. 5 ($\ln(\tau_E I_M/I_E)$ against $1/T$) the plots are linear; that is, one can write

$$\tau_E I_M/I_E = (\tau_E I_M/I_E)_0 \exp(-E_\eta^{\neq}/kT). \quad [9]$$

The slopes of the plots in Fig. 4 yield the values 61.2 and 62.2 kJ/mol for the activation energy $E_\eta^{\neq}$ of the microviscosity for TX100 and Tyloxapol micelles, respectively. Also represented in Fig. 5 are the semi-logarithmic variations of the lifetime τ_E of the DPP excimer with $1/T$. The plots are linear and yield the values 16.8 and 11.8 kJ/mol for the activation energy $E_{\tau E}^{\neq}$ of τ_E for TX100 and Tyloxapol.

For the sake of comparison we have also represented in Fig. 5 the variations of the values of τ_E and of the micellar microviscosity for the nonionic ethoxylated surfactant $C_{12}E_9$. It is seen that the microviscosity of $C_{12}E_9$ micelles is lower than that for TX100 and Tyloxapol micelles in the entire range of temperatures investigated. The activation energies for τ_E and

DOCKET ALARM

Explore Litigation Insights

Docket Alarm provides insights to develop a more informed litigation strategy and the peace of mind of knowing you're on top of things.

Real-Time Litigation Alerts

Keep your litigation team up-to-date with **real-time alerts** and advanced team management tools built for the enterprise, all while greatly reducing PACER spend.

Our comprehensive service means we can handle Federal, State, and Administrative courts across the country.

Advanced Docket Research

With over 230 million records, Docket Alarm's cloud-native docket research platform finds what other services can't. Coverage includes Federal, State, plus PTAB, TTAB, ITC and NLRB decisions, all in one place.

Identify arguments that have been successful in the past with full text, pinpoint searching. Link to case law cited within any court document via Fastcase.

Analytics At Your Fingertips

Learn what happened the last time a particular judge, opposing counsel or company faced cases similar to yours.

Advanced out-of-the-box PTAB and TTAB analytics are always at your fingertips.

API

Docket Alarm offers a powerful API (application programming interface) to developers that want to integrate case filings into their apps.

LAW FIRMS
Build custom dashboards for your attorneys and clients with live data direct from the court.

Automate many repetitive legal tasks like conflict checks, document management, and marketing.

FINANCIAL INSTITUTIONS
Litigation and bankruptcy checks for companies and debtors.

E-DISCOVERY AND LEGAL VENDORS
Sync your system to PACER to automate legal marketing.